Available online at www.sciencedirect.com
SCIENCE DIRECT®
Biosensors and Bioelectronics 20 (2005) 2181–2187
BIOSENSORS & BIOELECTRONICS
www.elsevier.com/locate/bios

Short communication

From MEMS to NEMS with carbon

Chunlei Wang*, Marc Madou

Department of Mechanical and Aerospace Engineering, University of California at Irvine, Irvine, CA 92697, USA

Received 23 June 2004; received in revised form 23 September 2004; accepted 23 September 2004
Available online 10 December 2004

Abstract

Our work in carbon-microelectromechanical systems (C-MEMS) suggests that C-MEMS might provide a very interesting material and microfabrication approach to battery miniaturization, active DNA arrays and a wide variety of chemical and biological sensors. In C-MEMS, photoresist is patterned by photolithography and subsequently pyrolyzed at high-temperatures in an oxygen-free environment. We established that it is possible to use C-MEMS to create very high-aspect ratio carbon structures (e.g. posts with an aspect ratio >10), suspended carbon plates and suspended carbon nanowires (C-NEMS). By changing the lithography conditions, soft and hard baking times and temperatures, additives to the resist, pyrolysis time, temperature and environment, C-MEMS permits a wide variety of interesting new MEMS and NEMS applications that employ structures having a wide variety of shapes, resistivities and mechanical properties. We also demonstrate that arrays of high-aspect ratio carbon posts can be charged/discharged with Li and this enables the fabrication of a smart switchable array of batteries.

Keywords: Carbon-microelectromechanical system (C-MEMS); Photoresist; Pyrolysis; High-aspect ratio; Suspended structure

1. Introduction

The reason Si today is one of the most commonly used micromachining materials is not only because of its excellent electronic and mechanical properties, the incredible degree of control one can exert over doping this semiconductor material and insulating its surface with SiO_2, but also because it has been the dominant material in the integrated circuit (IC) industry ever since the early 1950s. However, Si is not perfect for all applications. There are plenty of new demands that are challenging the continued dominance of Si and will require the introduction of new materials: increasing need for further miniaturization, higher speeds, better heat dissipation, lower power consumption and more environmentally friendly manufacturing processes. In the IC world, especially in micro-electromechanical systems (MEMS), many additional promising materials are used, including SiC, GaAs, quartz, polymeric materials and metals, depending on the specific application needs (Madou, 2002). Recently, microfabrication of carbon-based materials has received a lot of attention. Carbon comes in many forms: from diamond to graphite, buckeyballs, nanotubes, nanofibers, glassy carbon and diamond-like carbon (DLC). These materials are used in a variety of application fields, based on their widely differing crystalline structures and morphologies which enable very different physical, chemical, mechanical, thermal and electrical uses (Kroto et al., 1985; Ruland, 1990; Iijima, 1991). For example, glassy carbon electrodes are often used because of their wide electrochemical stability window, low-background and low-cost (Pocard et al., 1992). Graphite and hard carbons are well known for their utility in Li ion battery applications because of their Li intercalation/de-intercalation capacity (Eesenhard and Jurgen, 1999). Other properties, such as biocompatibility, chemically inertness and ease of functionalization have made carbon very attractive for biosensor and implantable device applications. One area, where carbon certainly meets several demands that Si cannot meet is in the area of biomimetics (life on earth is carbon-based, not silicon-based) and in the integration of man-made devices in living biological systems. Moreover, carbon nanotubes (CNTs) are of tremendous current interest in both fundamental research

* Corresponding author.
E-mail address: chunleiw@uci.edu (C. Wang).

0956-5663/$ – see front matter © 2004 Elsevier B.V. All rights reserved.
doi:10.1016/j.bios.2004.09.034

and for nanoelectronics applications including flat panel displays, chemical sensors and field emitters.

The development of carbon-microelectromechanical systems (C-MEMS) and carbon-nanoelectromechanical systems (C-NEMS) depends on lithographic patterning of resists (using any type of lithography) and their subsequent pyrolysis. For microfabrication of carbon structures, current processing technology, such as focused ion beam (FIB) (Irie et al., 2003) and reactive ion etching (RIE) (Tay et al., 2003) are time consuming and expensive because of the need of high-vacuum systems. Low feature resolution, and poor repeatability of the carbon composition as well as the widely varying properties of the resulting devices limits the application of screen-printing with commercial carbon inks for C-MEMS. Recently, more nontraditional carbon microfabrication methods were reported. Whitesides et al. described the use of soft lithography to fabricate glassy carbon microstructures. In this approach, micromolding of a resin such as poly(furfuryl alcohol) in an elastomeric mold yields polymeric microstructures, the microstructures are converted to free-standing carbon by heat treatment (500–1100 °C) in an inert atmosphere (Schueller et al., 1999). Another promising microfabrication technique is based on the pyrolysis of patterned resists at different temperatures and different ambient atmospheres (Madou et al., 1997; Kim et al., 1998). The electrochemical characteristics of carbon produced by pyrolysis of photoresists have been extensively studied (Kim et al., 1998).

They found that electrochemical reactions on pyrolyzed photoresist exhibit reaction kinetics very similar to those on glassy carbon. The advantage of using photoresists as the starting material for the microfabrication of various carbon structures is that the photoresists can be very finely patterned by lithography techniques and hence, a wide variety of repeatable shapes are possible. Moreover, different temperature treatments result in different resistivities and mechanical properties. Molecular rectification and conductance switching in pyrolyzed carbon-based molecular junctions were studied by McCreery et al. (2003), they found the current/voltage behavior showed strong and reproducible rectification and strong dependence on temperature and scan rate. Pyrolyzed photoresist carbon films were also demonstrated to be useful in electroanalytical and microfluidic applications; for example, pyrolyzed carbon has been used in conjunction with a microchip capillary electrophoretic device (Hebert et al., 2003).

Most pyrolyzed photoresist structures described in the literature today concern carbon features derived from positive photoresist and consist of very low aspect ratio structures (Ranganathan et al., 2000; Anariba et al., 2003). Here, we explore high-aspect ratio 3D carbon structures that will have a major impact on C-MEMS and MEMS in general. In this work, if we do not specifically mention it, C-MEMS always refers to the microfabrication of carbon by pyrolysis of photoresist. In the case of C-NEMS, it refers to the nanofabrication of carbon by pyrolysis and/or the integration of nanoscale materials and structures into C-MEMS devices.

2. Experimental

The fabrication of high-aspect ratio and high-density C-MEMS patterns is challenging because with increasing photoresist thicknesses, the requirements of any lithography process increase exponentially. In this work, C-MEMS structures were pyrolyzed from SU-8 negative tone photoresists, one of the most popular deep UV thick photoresists with very high-optical transparency, which makes it ideally suited for imaging near vertical sidewalls in very thick resist films. The C-MEMS fabrication process utilizes both UV photolithography and pyrolysis. The photolithography process includes the usual spin coating, soft-bake (not shown), near UV exposure, post-bake (not shown), and development. A typical process for a 200 μm thick SU-8 photoresist film involves spinning at approximately 500 rpm for 12 s then at 1400 rpm for 30 s, followed by a 10 min soft-bake at 65 °C and finally, a soft-bake for 80 min at 95 °C. Exposure was performed in a Karl Suss MJB3 contact aligner for about 100 s. The post-bake was carried out for 2 min at 65 °C and for 30 min at 95 °C. Development was carried out using a SU-8 developer from MicroChem (NANO^{TM} SU-8 developer). For SU-8 100 photoresist doped with iron oxide particles, an overexposure process was introduced with an exposure duration of as much as 5 min. Photoresist-derived C-MEMS architectures were obtained in a two-step pyrolysis process in an open ended quartz-tube furnace, in which samples were post-baked in a N_2 atmosphere at 300 °C for about 40 min first, then heated in a N_2 atmosphere (2000 sccm) up to 900 °C. At this point, the N_2 gas was shut off and forming gas [H_2 (5%)/N_2] was introduced (2000 sccm) for 1 h, then the heater was turned off and the samples were cooled down again in N_2 atmosphere to room temperature. The heating rate was about 10 °C/min, and the total cooling time was about 10 h.

Electrochemical measurements on C-MEMS posts were carried out using a three-electrode Teflon cell that employ an o-ring seal to define a working electrode area of ∼6.4 cm^2. The carbon electrode posts served as the working electrodes, while a lithium ribbon (99.9% pure, Aldrich) was used as both the counter and reference electrode. The electrolyte was 1 M $LiClO_4$ in a 1:1 volume mixture of ethylene carbonate (EC) and dimethyl carbonate (DMC). For the galvanostatic measurements, the current was based on the *C*/5 rate for graphite (corresponding to 50 and 580 μA for unpatterned and patterned films, respectively) and cells voltages varied between 10 mV and 1 V versus Li/Li$^+$.

3. Results and discussion

We have successfully made high-aspect ratio C-MEMS structures with aspect ratios larger than 10:1 using SU-8 negative photoresist by the just described two-step heating

process. A key point in the C-MEMS fabrication process is that, in order to maintain a CMEMS structure isometric to a given resist shape, one always needs to stay below the glass transition temperature (T_g) of the material that is being heated. The post-bake process cross-links the SU-8, enhancing adhesion of the resist to the substrate. That adhesion results in tensile stress in the carbon posts near the interface and the two-step heating process with its slow heating rate helps releasing this stress.

In Fig. 1(A) and (B), we show typical SU-8 patterns and carbon patterns derived from them. The average height of the SU-8 posts shown in Fig. 1(A) is around 300 μm. After pyrolysis, the overall shape of the cylindrical posts is largely retained, and a typical aspect ratio of the carbon post achieved is around 10:1. It was also found that the C-MEMS posts shrink much less near the base of the structures than at the midsection due to the good adhesion of SU-8 to the substrate. Shrinkage of the posts is also dependent on the overall height of the structure. For SU-8 posts with heights ranging from 100 to 350 μm, after pyrolysis, the corresponding carbon posts varied from 80 to 280 μm.

We demonstrated recently that the photoresist-derived high-aspect ratio C-MEMS posts could be charged and discharged with Li ions, providing a promising new material and microfabrication approach to battery miniaturization (Wang et al., 2004). Battery performance measurements on those samples show a large irreversible capacity on the first discharge followed by good subsequent cycling behavior, which is consistent with the behavior of coke materials used as lithium electrode materials. Galvanostatic charge/discharge cycling behavior and a cyclic voltammogram of a patterned carbon array are shown in Fig. 1(a) and (b) respectively. For a fully dense carbon film without any pattern, the capacity is 0.070 mAh cm^{-2} (~220 mAh g^{-1}) for the second and subsequent cycles. Furthermore, the normalized discharge current for a C-MEMS electrode array (180 × 180 posts with a post height of ~150 μm) was 0.125 mA cm^{-2} for the second and subsequent cycles, resulting in a nearly 80% higher capacity than that of the unpatterned carbon film.

The processes described above can easily be extended to two-level or multi-level C-MEMS structures. In the C-MEMS battery depicted in Fig. 2(a) one layer of carbon constitutes the current collector for the rows of anode and cathode posts

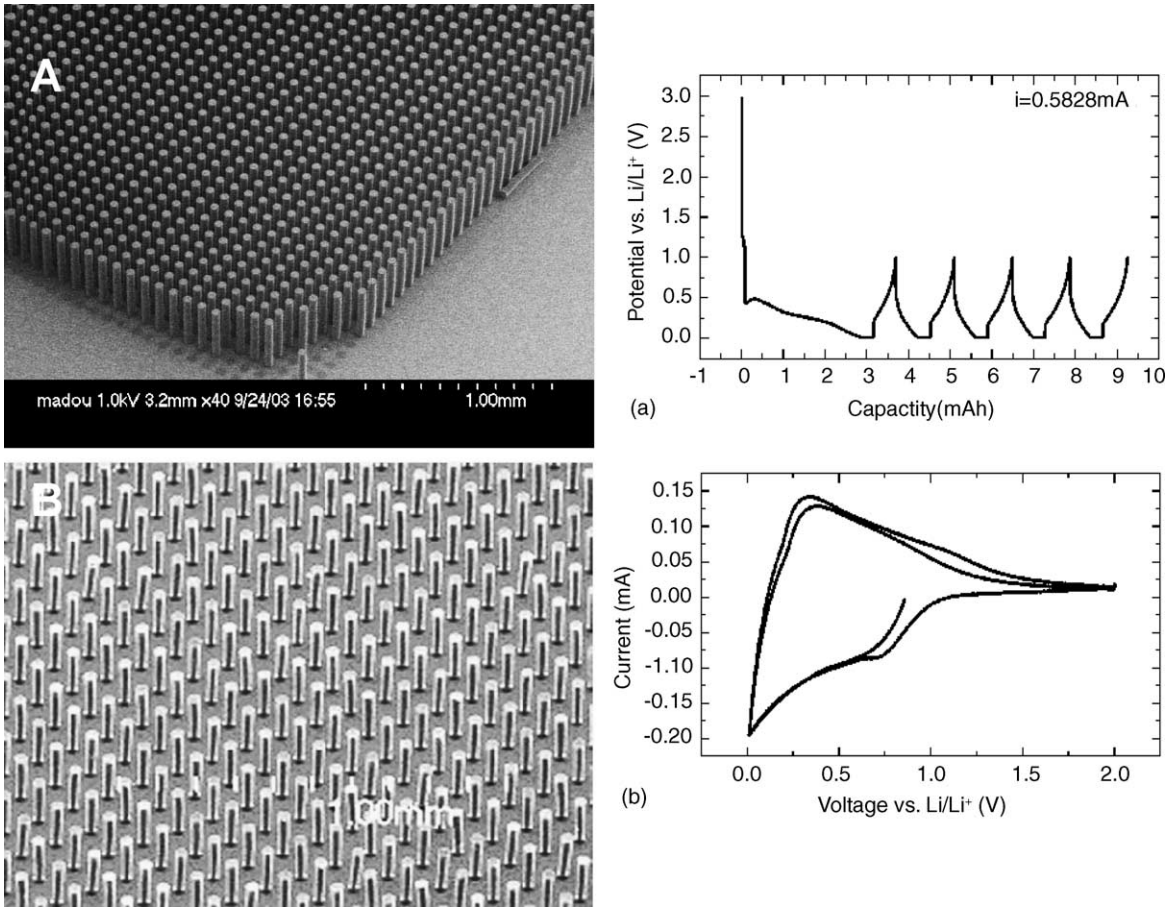

Fig. 1. Typical SEM images of (A) SU-8 post arrays (before pyrolysis) and (B) carbon post arrays (after pyrolysis). (a) Galvanostatic charge/discharge cycle behavior of patterned carbon arrays and (b) cyclic voltammetry of patterned carbon arrays.

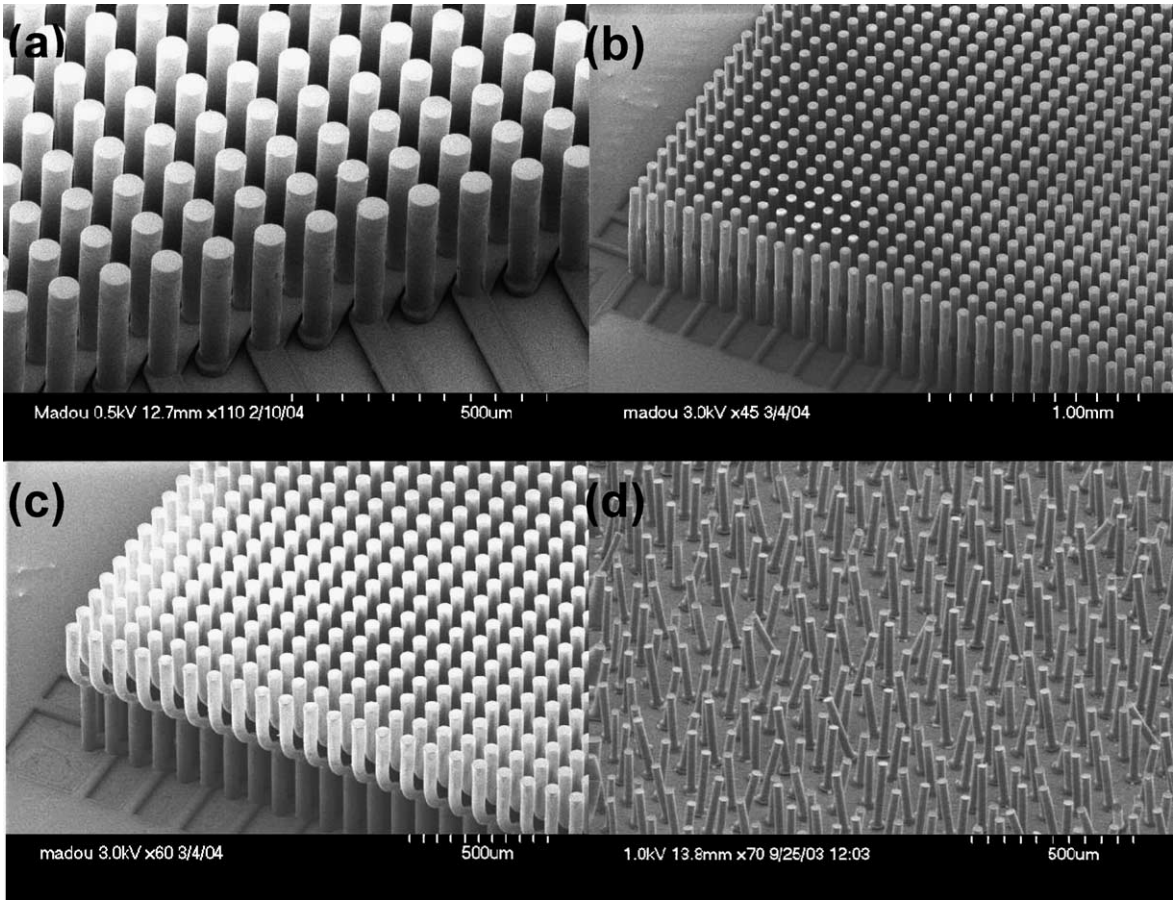

Fig. 2. Typical SEM images of (a) two-level SU-8 structure, (b) and (c) three-level SU-8 structure, and (d) carbon post arrays formed on Ti/Au layer.

in the second carbon layer. The advantages of using carbon as current collector include the excellent carbon–carbon adhesion and negligible contact resistance between carbon current collectors and carbon post arrays. Moreover, the processing of two-level C-MEMS can be easily achieved in one pyrolysis step. Using metal contacts, such as Ti/Au or Cr/Au, is impossible as during pyrolysis, the carbon posts are being pushed over due to formation of Au islands at high-temperatures, as shown in Fig. 2(d). In Fig. 2(a), we show a two-level SU-8 structure with a 20 μm thick current collector and 250 μm high-post arrays. In order to build yet higher aspect ratio (up to 40:1) C-MEMS structures, we developed a three-level C-MEMS process. In this process, each layer of SU-8 photoresist is exposed and baked separately, but the whole assembly is developed all at the same time in the last-step. Typical SEM photos of three-level C-MEMS devices are shown in Fig. 2(b) and (c). In Fig. 2(b), we show a three-level C-MEMS structure with all three-levels in good alignment. In Fig. 2(c), we show another three-level C-MEMS structure in good alignment but with the third level C-MEMS bending over maybe because of the relaxation of compressive stress caused by the photomask pushing against the top resist layer.

By carefully controlling the lithography processing parameters and the heating conditions, a variety of complex 3D C-MEMS structures, such as high-aspect C-MEMS posts and also suspended carbon wires, bridges, plates, and self-organized posts (carbon flowers) and ribbons (networks), were built. In the above described lithographic processing and optimization of SU-8 photoresist, the goal was to create high-aspect ratio posts with high-resolution and pattern transfer fidelity. In this section, we applied photoresist processing skills to form complicated suspended C-MEMS using non-traditional process recipes, such as overexposure, underdevelopment, directed flow of the developer and exploitation of surface tension in the developing photoresist patterns. Since we were able to make self-organized bunched C-MEMS posts (carbon flowers) repeatedly, we were encouraged to investigate in more detail suspended C-MEMS features. Suspended C-MEMS structures were frequently observed (see Fig. 3) and here we will explain how to make these structures intentionally.

Overexposure and different underdevelopment timing leads to suspended resist networks. During pyrolysis, uniform shrinkage of the photoresist network results in a suspended carbon network with increased openings as shown in Fig. 3(c). However, it is difficult to control the timing for underdevelopment because of its sensitivity to the photoresist thickness, exposure dose and baking condition. By using SU-8 photoresist doped with Fe_2O_3 nanoparticles, we

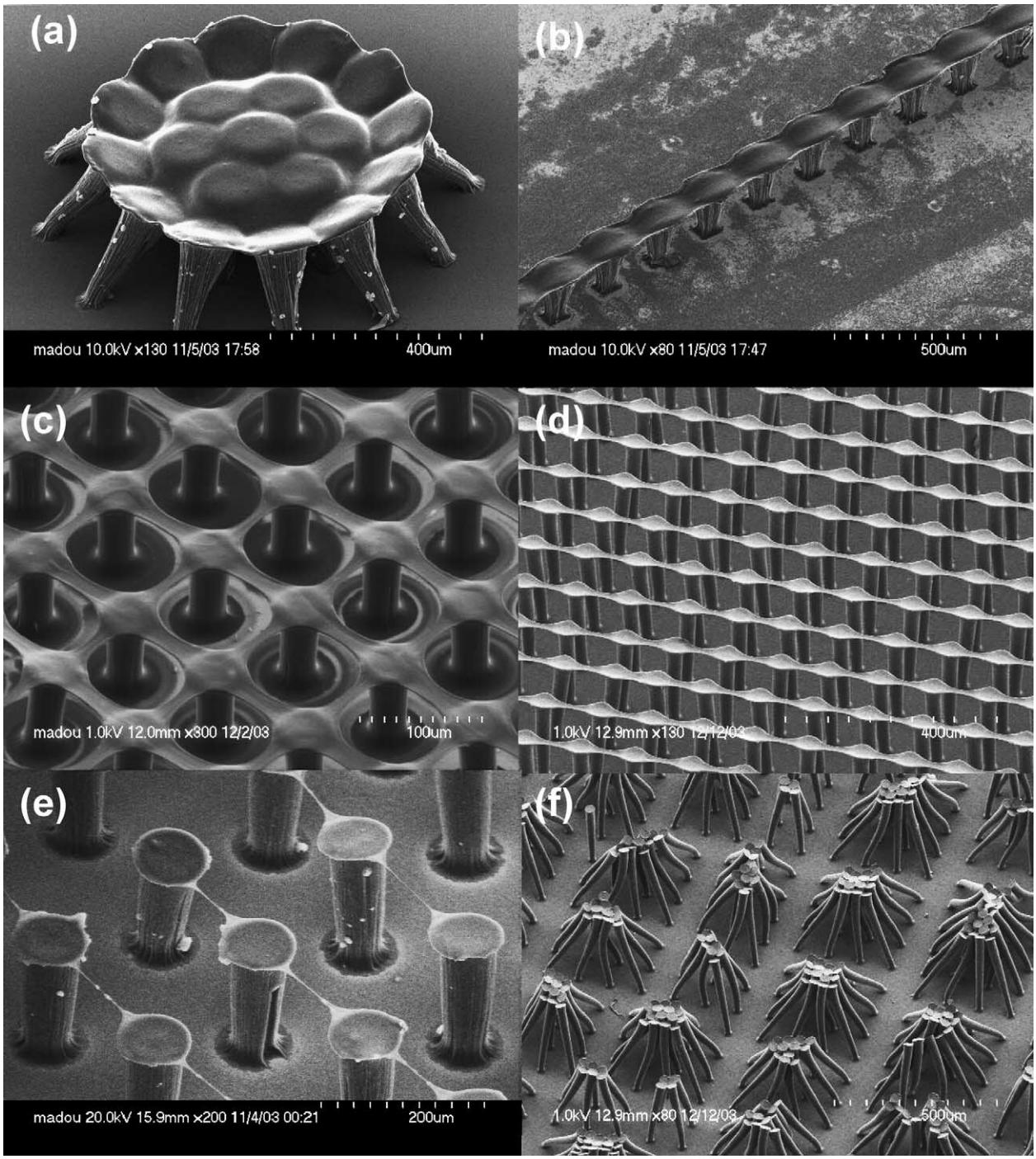

Fig. 3. Typical SEM images of suspended (a) carbon plates, (b) carbon bridge, (c) carbon networks, (d) carbon ribbons, (e) carbon fibers and (f) self-assembled C-MEMS.

found that we can control the formation of suspended structures much better. The modified SU-8 is dark brown, whereas undoped SU-8 is transparent, consequently thick colored resist requires significant longer overexposure times to transfer patterns, moreover, it leads to longer development times presenting more freedom to influence the final result. In the case of doped SU-8, the resist posts and derived carbon posts are much narrower at the bottom than at the top and appear fibrous because of the masking effect of individual or clustered nanoparticles (see, for example, Fig. 3(a) and (b)). The more open structure at the resist/substrate interface enables one to passively control the sideways flow of developer into the structure better. If suspended parts are desired, we oven-bake instead of baking on a hot plate to create the overhangs and underdevelop to avoid removing the overhangs and where we want to remove overhangs, we increase the development time.

By careful control of the geometric distribution of the posts in the array and the overexposure dose, a wide variety of beautiful and suspended C-MEMS structures, such as plates and bridges, as shown in Fig. 3(a) and (b), can be crafted. In order to improve the patterning quality and to shorten the processing time, both immersion and spray development were used to develop thick and dense SU-8 arrays. When the development speed of the immersion method started to slow down, we switched to spray development. By actively controlling the spray direction of developer to attack the exposed resist from one direction only (as opposed to the passive flow control described above), we can further control the resulting patterns to build, for example, ribbon like SU-8 structures. Suspended carbon ribbons after pyrolysis are shown in Fig. 3(d).

By proper control of the soft-bake, exposure and development time, suspended carbon fibers can also be built, as shown in Fig. 3(e). The diameter of the suspended carbon fibers obtained here is submicron. The wire resistance between two posts was measured at room temperature using two point probes, and a typical resistivity of $1.8 \times 10^{-2}\ \Omega\,\text{cm}$ was got.

In Fig. 3(f), we illustrate self-organized groups of carbon posts (bunched posts)—a feature most readily observed when starting with high-aspect ratio SU-8 arrays with posts higher than 300 μm. It should be noted that when bunching occurs, the bowed posts in each bunch remain structurally intact when converted to carbon. This means that the aggregation/bunching takes place after UV exposure, i.e., during post-bake, development, or during the drying after development. At the post-bake temperature, 'bunching' could in principle occur as the post-bake temperature (65 °C) is above the glass transition temperature of unexposed SU-8 (50–55 °C) and at those temperatures, the unexposed area reflows and this could enable the posts to move towards each other. From SEM observations, after the post-bake, the mask patterns are transferred with high fidelity, so clearly no aggregation/bunching is happening during post-bake. We also confirmed that by using too high-pressure on the nitrogen-drying gun, the developed high-aspect ratio post patterns randomly collapsed. The opportunity to control and optimize self-organized 2D textures obviously presents itself only during the development process itself. We speculate at this point that the dominant cause for the bunching of resist posts is surface tension. When the developer solution is removed this gently pulls posts that are tall and close enough together into symmetric patterns.

4. Conclusions

We have successfully made high-aspect ratio (>10:1) carbon posts by pyrolysis from negative photoresists in a simple one-step process. Electrochemical tests demonstrate that these C-MEMS electrodes can be charged/discharged with Li. A C-MEMS battery approach has the potential to solve both manufacturing and materials problems associated with microbatteries all at once. By careful control of processing parameters and heating conditions, a variety of complex 3D C-MEMS structures, such as suspended carbon wires, bridges, plates, self-organized bunched posts (carbon flowers) and networks, were demonstrated. Our work in C-MEMS suggests that C-MEMS might provide a very interesting material and microfabrication solution to the battery miniaturization problem, active DNA arrays and a wide variety of chemical and biological sensors.

Acknowledgements

The authors appreciate Ms. Lili Taherabadi, Mr. Guangyao Jia, Mr. Rabih Zaouk and Mr. Benjamin Park, Department of Mechanical and Aerospace Engineering, University of California at Irvine, for experiment assistance, Mr. Yuting Yeh and Prof. Bruce Dunn, Department of Materials Science and Engineering, University of California at Los Angeles, for Li intercalation into C-MEMS.

References

Anariba, F., DuVall, S., McCreery, R.L., 2003. Mono- and multilayer formation by diazonium reduction on carbon surfaces monitored with atomic force microscopy scratching. Anal. Chem. 75, 3837–3844.

Eesenhard, Jurgen, O. (Eds.), 1999. Handbook of Battery Materials. Wiley/VCH.

Hebert, N.E., Synder, B., McCreery, R.L., Kuhr, W.G., Brazill, S.A., 2003. Performance of pyrolyzed photoresist carbon films in a microchip capillary electrophoresis device with sinusoidal voltammetric detection. Anal. Chem. 75, 4265–4271.

Iijima, S., 1991. Helical microtubules of graphitic carbon. Nature 354, 56–58.

Irie, M., Endo, S., Wang, C.L., Ito, T., 2003. Fabrication and properties of lateral p-i-p structures using single crystalline CVD diamond layers for high electric field applications. Diam. Relat. Mater. 12, 1563–1568.

Kim, J., Song, X., Kinoshita, K., Madou, M., White, R., 1998. Electrochemical studies of carbon films from pyrolyzed photoresist. J. Electrochem. Soc. 145, 2314–2319.

Kroto, H.W., Heath, J.R., Brien, S.C.O., Curl, R.F., Smalley, R.E., 1985. C60: buckminsterfullerene. Nature 318, 162–163.

Madou, M., 2002. Fundamentals of Microfabrication: The Science of Miniaturization, 2nd ed. CRC Press.

Madou, M., Lai, A., Schmidt, G., Song, X., Kinoshita, K., Fendorf, M., Zettl, A., White, R., 1997. Chemical and biological sensors and analytical electrochemical methods. In: Ricco, A., Butler, M., Vanysck, P., Horvai, G., Silva, A. (Eds.), The Electrochemical Society Proceedings Series, vol. PV97-19, Pennington, NJ, p. 61.

McCreery, R., Dieringer, J., Solak, A.O., Snyder, B., Nowak, A.M., McGovern, W.R., DuVall, S., 2003. Molecular rectification and conductance switching in carbon-based molecular junctions by structural rearrangement accompanying electron injection. JACS 125, 10748–10758.

Pocard, N.L., Alsmeyer, D.C., McCreery, R.L., Neenan, T.X., Callstrom, M.R., 1992. Doped glassy carbon: a new material for electrocatalysis. J. Mater. Chem. 2 (8), 771–784.

Ranganathan, S., McCreey, R., Majji, S.M., Madou, M., 2000. Photoresist-derived carbon for microelectromechanical systems and

electrochemical applications. J. Electrochem. Soc. 147, 277–282.
Ruland, W., 1990. Carbon-fibers. Adv. Mater. 2, 528–536.
Schueller, O.J.A., Brittain, S.T., Whitesides, G.M., 1999. Fabrication of glassy carbon microstructures by soft lithography. Sens. Actuators A:Phys. 72, 125–139.
Tay, B.K., Sheeja, D., Yu, L.J., 2003. On stress reduction of tetrahedral amorphous carbon films for moving mechanical assemblies. Diam. Relat. Mater. 12, 185–194.
Wang, C.L., Taherabadi, L., Jia, G., Madou, M., Yeh, Y., Dunn, B., 2004. Electrochem. Solid-State Lett. 7 (11), A435–A438.